Periodically Clickable Polyesters: Study of Intrachain Self-Segregation Induced Folding, Crystallization, and Mesophase Formation

ARTICLE *in* JOURNAL OF THE AMERICAN CHEMICAL SOCIETY · JANUARY 2014

Impact Factor: 12.11 · DOI: 10.1021/ja411583f · Source: PubMed

4 AUTHORS, INCLUDING:

Joydeb Mandal
Indian Institute of Science
2 PUBLICATIONS **7** CITATIONS
SEE PROFILE

Kris Prasad
Centre for Nano and Soft Matter Sciences
295 PUBLICATIONS **2,950** CITATIONS
SEE PROFILE

JACS
JOURNAL OF THE AMERICAN CHEMICAL SOCIETY

Article

pubs.acs.org/JACS

Periodically Clickable Polyesters: Study of Intrachain Self-Segregation Induced Folding, Crystallization, and Mesophase Formation

Joydeb Mandal,[†] S. Krishna Prasad,[#] D. S. Shankar Rao,[#] and S. Ramakrishnan*[,†]

[†]Department of Inorganic and Physical Chemistry, Indian Institute of Science, Bangalore-560012, India
[#]Center for Soft Matter Research, Bangalore-560013, India

Supporting Information

ABSTRACT: A series of polyesters based on 2-propargyl-1,3-propanediol or 2,2-dipropargyl-1,3-propanediol or 2-allyl-2-propargyl-1,3-propanediol and 1,20-eicosanedioic acid were prepared by solution polycondensation using the corresponding diacid chloride; these polyesters were quantitatively "clicked" with a fluoroalkyl azide, namely $CF_3(CF_2)_7CH_2CH_2N_3$, to yield polyesters carrying long-chain alkylene segments in the backbone and either one or two perfluoroalkyl segments located at periodic intervals along the polymer chain. The immiscibility of the alkylene and fluoroalkyl segments causes the polymer chains to fold in a zigzag fashion to facilitate the segregation of these segments; the folded chains further organize in the solid state to form a lamellar structure with alternating domains of alkyl (HC) and fluoroalkyl (FC) segments. Evidence for the self-segregation is provided by DSC, SAXS, WAXS, and TEM studies; in two of the samples, the DSC thermograms showed two distinct endotherms associated with the melting of the individual domains, while the WAXS patterns confirm the existence of two separate peaks corresponding to the interchain distances within the crystalline lattices of the HC and FC domains. SAXS data, on the other hand, reveal the formation of an extended lamellar morphology with an interlamellar spacing that matches reasonably well with those estimated from TEM studies. Interestingly, a smectic-type liquid crystalline phase is observed at temperatures between the two melting transitions. These systems present a unique opportunity to develop interesting nanostructured polymeric materials with precise control over both the domain size and morphology; importantly, the domain sizes are far smaller than those typically observed in traditional block copolymers.

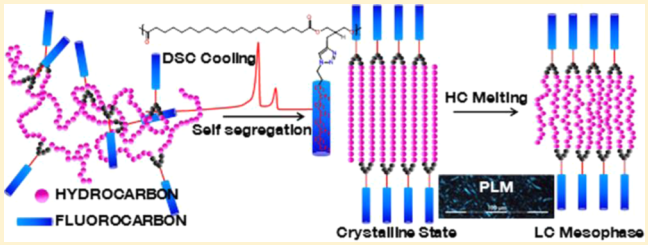

INTRODUCTION

Segmented polymers of different types carrying two or more immiscible segments tend to self-segregate, leading to the emergence of several interesting properties, in materials such as thermoplastic elastomeric polyurethanes, liquid crystalline polymers, nanostructured polymeric films, etc. These segmented polymers can be of several types, such as block copolymers (di, tri, and multi) and graft copolymers, in addition to other topological variations of these, such as star block copolymers, etc. When the length of the segments and the periodicity of their placement are precisely controlled, well-defined and predictable morphologies are seen; however, when both of these features are ill-defined, then randomly phase-separated systems emerge, which, despite the randomness, can yield remarkably useful properties, such as in the case of thermoplastic polyurethanes.

Precise control of segment sizes has been most effectively demonstrated in the case of block copolymers; first, they were prepared using anionic living polymerization methods[1] but more recently using a variety of interesting controlled radical polymerizations.[2] Achieving the same level of precision in the segment sizes in graft copolymers is a far more difficult task; while the length of the grafted segment is a relatively easy parameter to control, the periodicity of grafting is a far more challenging task. The former has been best achieved using the "graft-onto" and macromonomer approaches, both of which utilize living polymerization methods to control the graft-segment length.[3] The periodic placement of the grafted segment, on the other hand, requires precise control over the location of functional groups (graft-anchoring locations) along a polymer backbone, which is a far more difficult task; Mays, Hadjichristidis, and others have developed some interesting approaches to prepare "exact" graft copolymers wherein greater control over the periodicity of the graft junctions has been achieved.[4] Some progress has also been made to achieve improved control of the location of comonomers during polymerization by periodic dosing of comonomers during a controlled radical polymerization process;[5] although not precise, this process greatly helps to reduce the dispersity in the locations of the comonomers and could clearly become a potential approach to prepare periodically grafted polymers.

Received: November 13, 2013
Published: January 16, 2014

dx.doi.org/10.1021/ja411583f | J. Am. Chem. Soc. 2014, 136, 2538−2545

The most effective methodology to locate functional groups at precise distances along a polymer backbone would be to use condensation polymerization methods, as was demonstrated by Wagener and co-workers using ADMET polymerization.[6] The above two approaches are truly complementary; the former approach would be less precise, but technically there are no intrinsic limitations to the achievable periodicity, i.e., the segment length between grafting points. On the other hand, while the condensation approaches are very precise, it becomes increasingly difficult when the segment length between the adjacent functional groups becomes large.

Chain folding during the crystallization of polyethylene (PE) has been extensively studied for decades; in particular, the role of random branching (or *defects*) on the crystallization of PE has been thoroughly examined.[7] Control of the precise location of the "defect" along a polymer backbone has been utilized as an excellent method to regulate the chain-folding during the crystallization of polyethylene-like polymers; thus, control over both the dimension of the lamellae and the nature of groups located on the surface has been achieved. Whereas ADMET chemistry has been extensively used to locate a variety of functional groups and *fold-inducing* segments at precise locations to study their effect on the crystal morphology of pure hydrocarbon-based backbones,[8] polyethylene-like polyesters have also been prepared using traditional condensation routes utilizing long-chain diols to regulate the periodicity.[9] When long alkane diols are used, a lamellar morphology similar to those seen in polyethylene is observed due to the exclusion of the bulky substituent located on the short diacid fragment; the thickness of the lamellae was thus regulated by the periodicity of the defect.[9]

In most of the earlier studies, the primary objective was to explore the use of periodically located *defects*, that exclude the paraffinic crystalline lattice, to regulate the thickness of the folded lamellae. Recently, we designed a polyethylene-like polyester, wherein long hydrophilic PEG chains were periodically located along a hydrophobic polyester backbone;[10] it was shown that these polymer chains fold in a zigzag fashion in a polar solvent, and the folded form is further stabilized by the crystallization of the intervening alkylene segment (>C12), to form what we termed "PEGylated wax-like nanobundles". Extremely uniform plate-like aggregates were seen in the AFM images of spin-cast films; the thickness of these flat aggregates matched the estimated height of the anticipated folded chains. In our previous approach, PEGylated diethyl malonate was used as one of the monomers and was condensed with long-chain diols; it therefore lacked the design flexibility to place any desired segment at periodic intervals. In an effort to develop a more general strategy to prepare periodically functionalizable polyesters, we report here the preparation of *clickable* polyesters carrying propargyl/allyl functionality at regular intervals along the polymer backbone; thus, using a single polyester, different desired segments can be quantitatively clicked to address interesting questions about the behavior of such *precisely grafted copolymers*. Specifically, we have prepared polyesters, carrying either one propargyl, two propargyls, or both a propargyl and an allyl group at regular intervals, using suitably designed diols (Scheme 1); these polyesters were then clicked with fluoroalkyl azides to generate three types of systems that carry either one or two fluoroalkyl chains at periodic intervals. Fluoroalkyl chains were specifically chosen to examine the immiscibility-driven chain folding and the consequent formation of a lamellar morphology; importantly, given the strong tendency of the fluoroalkyl chains to crystallize, we wished to explore the possibility of independent crystallization of both the backbone and the pendant chains. The polymers were characterized using a variety of techniques, including DSC, SAXS, and TEM, to examine the self-segregation of alkylene (HC) and fluoroalkyl (FC) segments; a remarkable observation was the anticipated independent crystallization of the HC and FC segments, which is most readily possible if the polymer chains fold in the anticipated zigzag fashion.

Scheme 1. Synthesis of Periodically Clickable Polyesters

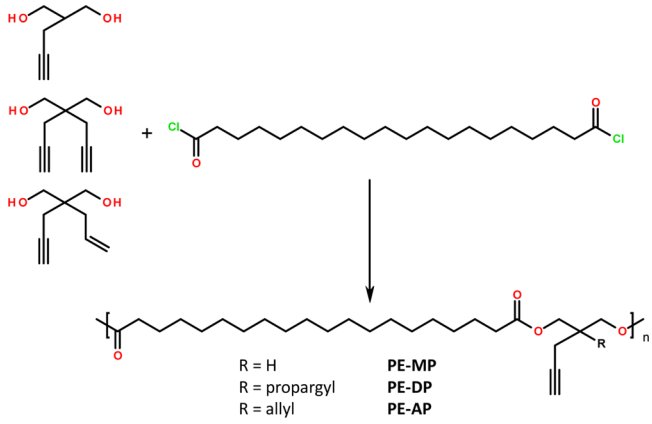

RESULTS AND DISCUSSION

Because our primary objective was to prepare clickable polyethylene-like polyesters carrying long alkylene segments along the polymer backbone, we initially examined the possibility of using diethyl malonate-based monomers along with 1,20-eicosanediol; to achieve this, we prepared diethyl 2-propargylmalonate and attempted melt-transesterification with eicosanediol. However, we found that the transesterification was very sluggish and, in the case of the 2,2-dipropargylmalonate derivative, no reaction occurred, suggesting that substitution at the 2-position of the diethyl malonate drastically reduces the reactivity of the diester. Therefore, we instead chose to reduce the diethyl malonate after alkylation with the required moiety, namely a single propargyl, two propargyls, or a propargyl and an allyl unit, to yield different clickable diols. As shown in Scheme 1, condensation of these diols with the eicosanedioic acid chloride in the presence of pyridine yielded the required polyesters carrying periodically clickable propargyl and/or allyl moieties. The polyesters were isolated after purification by three reprecipitations using chloroform/methanol.

The proton NMR spectra of the three polymers are shown in Figure 1. From the NMR spectra, it is clear that peaks associated with the possible end-groups were essentially absent (Figure S1, Supporting Information), suggesting the formation of moderate molecular weight polymers in all cases. The molecular weights of the parent polyesters were estimated by GPC (against narrow polystyrene standards) using chloroform as the eluent; the molecular weights were found to be moderately high with M_n values ranging from 12 000 to 28 000 (Figure S2, Supporting Information). Other features in the NMR spectra of the samples were in complete accordance with the expected structure, as evident from the peak assignments shown in the figure; HETCOR spectrum of one of the samples, PE-MP (Figure S3, Supporting Information), was measured to confirm the assignment. In order to place hydrocarbon-

dx.doi.org/10.1021/ja411583f | J. Am. Chem. Soc. 2014, 136, 2538−2545

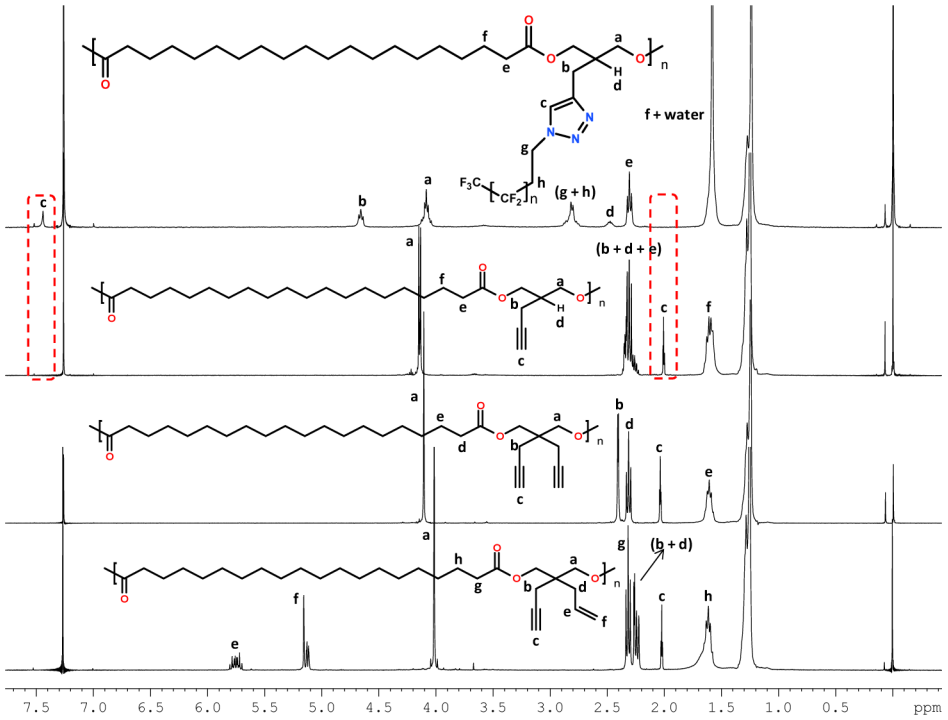

Figure 1. ^{1}H NMR spectra of the three parent polyesters and that of one representative fluoroalkyl-clicked polymer, PE-MP-F; the spectra were recorded in $CDCl_3$.

immiscible segments at periodic intervals, we chose to click a fluoroalkyl (FC) segment using the azide $CF_3(CF_2)_7CH_2CH_2N_3$, which was prepared from the corresponding commercially available iodide. The NMR spectra of the clicked polymers clearly confirmed quantitative reaction; a representative spectrum of the clicked polymer, PE-MP-F, is shown in Figure 1, which shows the complete disappearance of the peak associated with the pendant propargyl group (~2.0 ppm) and the appearance of a peak associated with the triazole ring proton (~7.5 ppm). The same was true for the other two samples also, as evident from their NMR spectra (Figure S4, Supporting Information). The FC segment was selected for two reasons: one is its immiscibility with the backbone alkyl segment, which should promote self-segregation; the second important reason was to examine whether the FC segments could also crystallize independently. Segregation of FC and hydrocarbon (HC) has been studied in simple small molecule amphiphiles[11] as well as in suitably designed polymers;[12] in some specific systems the segregation was also shown to lead to the formation of a smectic-type liquid crystalline phase.[13] One of the objectives of preparing the polymer carrying both propargyl and allyl groups, namely PE-AP, was to anchor two different segments orthogonally; however, our efforts to click a PEG unit using the thiol−ene reaction, subsequent to clicking the FC segment, failed. This inability to place PEG units, we believe, could be due to the inaccessibility of the allyl site to the PEG-SH, once the FC segment has been installed; this may be because of the occurrence of self-segregation-induced folding in the reaction medium, which in turn restricts the access of a relatively polar PEG-SH to the allyl site which may be buried within the FC domain.

Thermal Analysis. The first evidence for the self-segregation-induced domain formation in the bulk sample can be seen from the DSC thermograms (Figure 2); in both PE-MP-F and PE-DP-F samples, two clear endothermic transitions are visible, while in the case of PE-AP-F only a single transition is seen during the heating run, but a shoulder alongside the main exothermic peak is visible during the cooling scan. All the thermograms were measured using a heating/cooling rate of 10 deg/min, and they were completely reproducible as confirmed from the overlapping of the second and third scans (Figure S5, Supporting Information).

It is well-known that fluorocarbon segments behave as relatively stiff units and exhibit a strong tendency to crystallize;[13,14] therefore, if the proposed self-segregation by folding of the polymer chains (as depicted in Figure 2) were to occur, then one might expect independent melting transitions associated with the HC and FC phases. Upon inspection of the relative intensities of the two peaks in samples PE-MP-F and PE-DP-F, it is clear that the relative intensity of the higher temperature peak is substantially more for PE-DP-F, which carries two pendant fluoroalkyl chains per repeat unit. It appears reasonable, therefore, to ascribe the higher temperature peak to the melting of the FC domain and the lower temperature peak to that of the HC domain. Assuming this to be the case, the enthalpies associated with the individual peaks were normalized with respect to the weight-fraction of the appropriate segment, and these values are listed in the figure. A few important points emerge from the DSC studies: (i) the transition temperatures vary significantly from one sample to the other, even though they are presumed to be associated with the same FC or HC phases; (ii) while only a small change in the segment-normalized enthalpy of the peak associated with the FC domain is seen (12 to 14 mJ/mg), there is a substantial change in the value associated with the peak corresponding to the HC domain (99 to 57 mJ/mg). The FC chains are known to adopt a twisted helical conformation in the crystalline phase,[15] and consequently it may be expected that the presence of two FC segments on each repeat unit would hinder the effective close packing of the HC chains in the

dx.doi.org/10.1021/ja411583f | J. Am. Chem. Soc. 2014, 136, 2538−2545

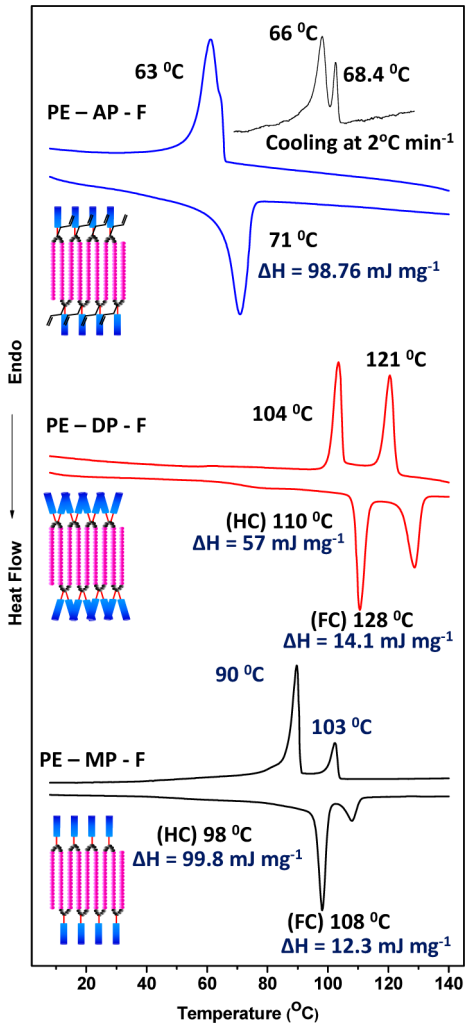

Figure 2. DSC thermograms of the various clicked polyesters; the scans were performed at a heating/cooling rate of 10 deg/min. The enthalpies associated with the transitions, in the case of PE-MP-F and PE-DP-F, were normalized with respect to the weight-fraction of the segment associated with the specific transition. The inset in the top panel is of the slow cooling scan performed at 2 deg/min, which reveals the presence of two distinct transitions even in the case of PE-AP-F.

polymer backbone. In the case of PE-AP-F, the presence of the allyl group clearly appears to hinder the crystallization of the FC segments, thereby lowering its melting peak and causing a merger of the two peaks associated with the FC and HC domains; however, the slow cooling scan (at 2 deg/min) revealed the presence of two distinct peaks (see Figure 2), confirming the occurrence of self-segregation in this sample as well. One other intriguing observation is the apparent stabilization of the HC phase in PE-DP-F, as reflected by the significantly higher melting temperature of the HC domain (104 °C vs 90 °C), this despite the much lower normalized enthalpy associated with this peak.

Earlier studies by Wilson and Griffin on polymers carrying both FC and HC segments have suggested the existence of a smectic-type mesophase;[13] they too had hypothesized the self-segregation of the two domains leading to the possible formation of a lamellar morphology. Polarizing light microscopic (PLM) studies of the samples revealed that both PE-MP-F and PE-DP-F exhibit birefringence and fluidity in the

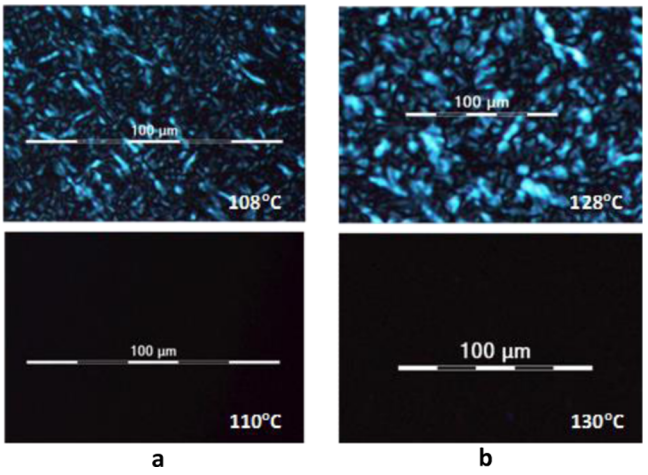

Figure 3. Polarizing light microscopic images of PE-MP-F (a) and PE-DP-F (b) in the mesophase and in the isotropic phase. Shearing the sample was readily possible in the mesophase.

temperature region between the two endothermic peaks (Figures 3, and Figure S6, Supporting Information). The birefringent patterns disappear above the clearing temperature but remain frozen in the solid thin films at room temperature. These observations confirm the formation of a mesophase, similar to those observed by Wilson and Griffin[13] but in a distinctly different class of polymers, thus reaffirming that the presence of two immiscible segments, with molecular dimensions, having different melting temperatures is adequate for the observation of a liquid crystalline phase. A schematic depiction of the process leading to the formation of the liquid crystalline phase in our periodically grafted copolymers is shown in Scheme 2.

X-ray Scattering Studies. The formation of lamellar morphology is readily confirmed from small-angle X-ray scattering (SAXS); the SAXS profile of PE-MP-F clearly reveals multiple scattering peaks that provides evidence for the formation of highly ordered lamellar organization, with peaks up to the fifth order readily visible. Evidently, the presence of the alternating domains of fluorocarbon (FC) and hydrocarbon (HC) segments provides a clear segregation leading to well-defined layering. Variable temperature SAXS studies were carried out by cooling the samples from melt and recording data at various temperatures, after thermal equilibration; the data is presented in Figure 4. First, it is interesting to note that the peaks are considerably sharper at 92 °C than at 26 °C, suggesting that there appears to be a refinement of the self-segregation and ordering prior to the first melting transition; this is also reflected in the distinct sharpening of the peaks in the wide angle region prior to melting (Figure S7, Supporting Information). Furthermore, on cooling from 96 °C to 92 °C, there is an abrupt increase in the *d*-spacing from 5.12 to 5.81 nm; this is apparently from the ordering of the HC domains due to crystallization. At 110 °C, i.e., above the second melting peak in the DSC, the lamellar ordering is completely absent. The temperature at which this ordering occurs is consistent with the first crystallization peak in the DSC thermogram (onset at ∼104 °C) during the cooling scan. Similar variations are also seen in the case of the PE-DP-F sample; at 135 °C the lamellar ordering is absent and, just as in the previous sample, the ordering occurs immediately upon crystallization (DSC onset at ∼124 °C) of the FC domains. The interlamellar

dx.doi.org/10.1021/ja411583f | J. Am. Chem. Soc. 2014, 136, 2538−2545

Scheme 2. Immiscibility-Driven Self-Segregation of the HC and FC Segments by Folding of a Polymer Chain[a]

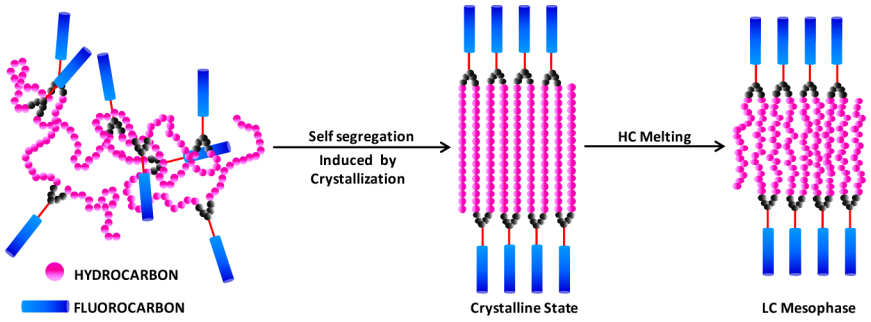

[a]Once the HC and FC segments are colocated, they crystallize independently to generate a lamellar morphology. Melting of the HC domain (in magenta) leads to the formation of a smectic-type liquid crystalline phase; the fluidity comes from the molten nature of the alternate HC domains.

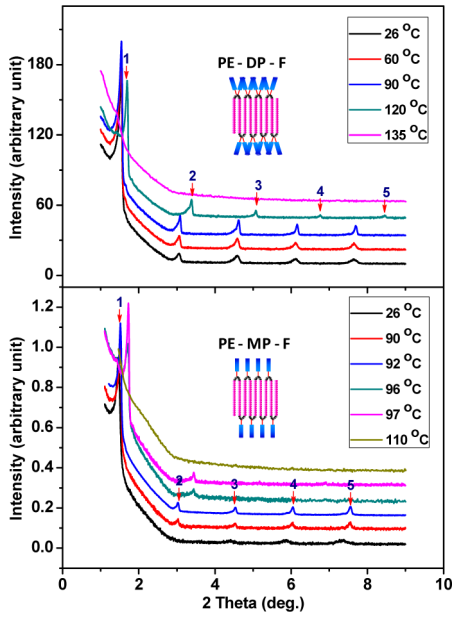

Figure 4. Variation of SAXS profile of PE-MP-F and PE-DP-F as a function of temperature. Samples were heated to an isotropic state and cooled; the SAXS data were collected after equilibration at each temperature for ~10 min.

spacing increases from 5.2 nm at 120 °C to 5.71 nm at 90 °C, which is below the second crystallization peak in the DSC (peak maximum at ~104 °C). Interestingly, in PE-DP-F extended lamellar ordering appears to have been attained even at 120 °C, i.e., before the crystallization of HC domains. Lamellar ordering is also seen in sample PE-AP-F but is less developed; the interlamellar spacing is about 5.6 nm at 26 °C, which disappears at 80 °C (Figure S8, Supporting Information), again consistent with the single melting transition seen in the DSC thermogram.

In summary, the variable temperature SAXS studies reveal that, during the cooling of the isotropic melt, the lamellar ordering begins immediately upon crystallization of the FC domains and becomes more extended once the HC domains also crystallize; importantly, crystallization of both domains causes a slight increase in the interlamellar spacing, presumably due to the chain extension that occurs when the backbone alkylene segment adopts an all-trans conformation. Molecular modeling of representative FC-HC-FC triblock structures bearing the appropriate linking segments (Figure S9, Supporting Information) provided an estimate of the end-to-end distance, which ranged from 6.50 to 6.67 nm; this is larger than the observed range of ~5.6–5.8 nm. This difference can be attributed to one of several factors, namely the conformation of the linker, presence of gauche defects, partial interdigitation of the FC segments, and/or a tilt in the alkylene segment with respect to the smectic layer normal.

The wide angle region of the X-ray scattering profiles for the three samples is shown in Figure 5. All the samples exhibit two

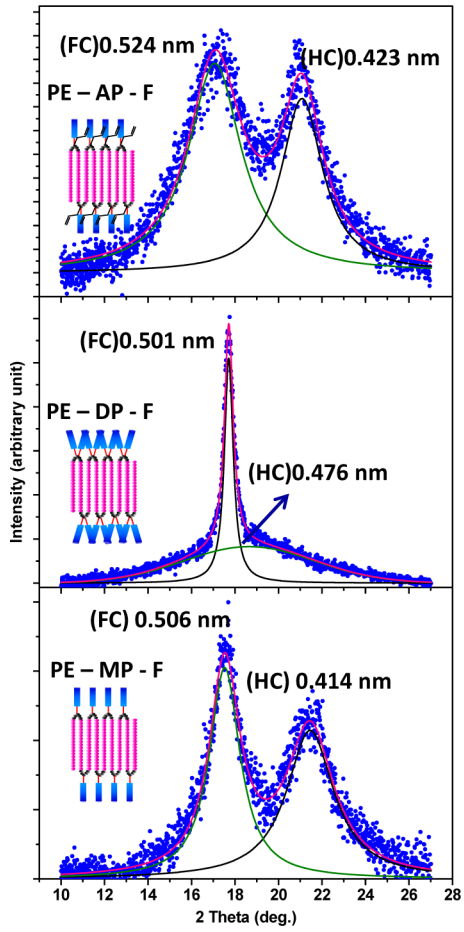

Figure 5. WAXS profiles for PE-MP-F, PE-DP-F, and PE-AP-F; the higher angle peak is due to the interchain spacing within the crystalline lattice of the hydrocarbon (HC) domain, while the the lower angle peak is due to spacing between the fluorocarbon chains within the crystalline lattice of the FC domain.

dx.doi.org/10.1021/ja411583f | J. Am. Chem. Soc. 2014, 136, 2538–2545

peaks, although the second peak is much broader and less distinct in the PE-DP-F sample. Deconvolution of scattering profiles provided the *d*-spacings corresponding to the two peaks, and these values are listed in the figure; the peak at ∼0.414 nm in PE-MP-F corresponds to the interchain spacing within the hydrocarbon layer, while that at ∼0.506 nm corresponds to the interchain spacing within the fluorocarbon domain. These values match well with those typically reported for the crystalline phases formed by alkyl and fluoroalkyl chains.[16b] In the sample carrying two fluoroalkyl chains per repeat unit, PE-DP-F, a remarkably sharp peak is seen corresponding to a spacing of 0.501 nm, reflecting the interchain distance between fluoroalkyl chains within the crystalline FC domain, along with a broad peak corresponding to a *d*-spacing of 0.476 nm; this broad peak with a significantly higher spacing reflects the poor packing within the HC domain, an aspect that we will revisit later. In PE-AP-F, on the other hand, two clear peaks are seen; the *d*-spacings associated with both the FC and HC domains in this case are significantly larger (0.524 and 0.423 nm, respectively), suggesting a less compact organization within both the layers. The variation of the WAXS profiles as a function of temperature (Figure S7, Supporting Information) is generally consistent with the observations made in the small-angle region; first, in PE-MP-F, there is a distinct sharpening of the peak associated with the HC domains with an increase in temperature. This sharpening suggests a more homogeneous ordering within both layers. Importantly, in both PE-MP-F and PE-DP-F, the peak associated with the HC domain vanishes at a temperature above the first melting transition, confirming that the low temperature peak is indeed associated with the melting of the backbone alkylene segment.

Electron Microscopy. The presence of alternating layers of fluorocarbon and hydrocarbon segments should provide adequate contrast for direct visualization using TEM. Samples for TEM studies were prepared by drop-casting dilute chloroform solution (0.25 mg/mL) of the polymers on a carbon-coated Cu grid (400 mesh). Dark-field TEM images provided significantly better contrast than the bright-field ones; the dark-field images of PE-MP-F and PE-DP-F are shown in Figure 6. It is evident that in both cases well-defined lamellae are visible; the selected area electron diffraction (SAED) pattern clearly reveals that the interlamellar spacing in PE-MP-F is about 5.5 nm, while in PE-DP-F it is slightly lower, about 5.25 nm (Figure S10, Supporting Information). Both of these values are slightly smaller than the estimates obtained from SAXS data; however, in accordance with the X-ray data, here too the interlamellar spacing estimated for PE-MP-F is slightly higher than that of PE-DP-F. One other intriguing feature seen in some regions of the image, in the case of PE-DP-F, is the higher level periodicity that corresponds to a spacing of 21 nm, which is four times the interlamellar spacing (Figure 6); it is interesting that a similar higher order periodicity in the TEM images was earlier observed by Hopken and Möller[11d] and was ascribed to the rolling-up of a double bilayer to form cylinders whose diameter would be four times that of the interlamellar spacing.

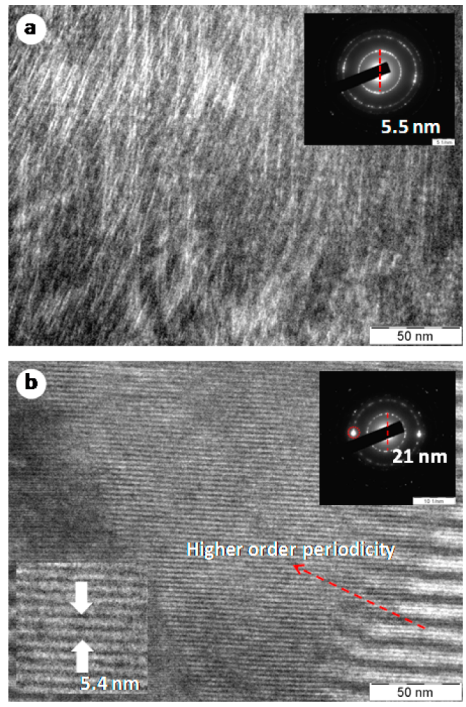

Figure 6. TEM images of PE-MP-Fand PE-DP-F. (a) Dark-field image of PE-MP-F along with the inset showing the SAED pattern. (b) Dark-field image of PE-DP-F showing the presence of two regions: one where the higher order periodicity is reflected by the SAED pattern, and the other as shown in the expanded image shows a lower periodicity of ∼5.4 nm.

DISCUSSION

Polymers carrying long aliphatic hydrocarbon and fluorocarbon segments have been extensively studied, in particular, to understand the consequence of smectic ordering on the wetting characteristics.[17] In majority of the studies, polymers carrying pedant groups bearing alkyl-fluoroalkyl segments, such as $(CH_2)_n(CF_2)_mCF_3$, have been examined; the role of the values of *n* and *m* in governing the phase separation and smectic mesophase formation and their effect on the wetting behavior were studied.[18] There are only two reports, thus far, by Wilson and Griffin, on polymers bearing polymethylene segments along the backbone and fluoroalkyl groups as pendant units, which appeared over two decades ago;[13] they too had invoked the self-segregation of the FC and HC segments to explain the LC behavior of their polymers. However, no experimental confirmation of the molecular structural origins for the formation of the mesophase was provided. On the basis of all the observations thus far, it has been inferred that single polymer chains undergo an *immiscibility-driven folding to permit the self-segregation of the HC and FC segments*, as depicted in Scheme 2; these folded chains then organize in the solid state to generate a lamellar morphology. Once the two different segments collocate, they crystallize independently, as evident from the two melting transitions in the DSC scans; at temperatures between the two melting transitions, a smectic-type mesophase that can be readily sheared is exhibited. This is in contrast to the model proposed by Wilson et al., where they have postulated that the polymethylene segments undergo a hairpin bend to account for their SAXS data.[19]

To gain more structural evidence for our hypothesis that the individual peaks reflect the melting of the HC and FC domains, we carried out variable temperature IR spectroscopic measurements. It is well-known that the melting of a crystalline paraffinic lattice containing extended all-trans alkyl chains causes a shift of the peaks associated with the symmetric and asymmetric C−H stretching vibrations. For an all-trans alkyl chain, as in crystalline *n*-alkanes, the symmetric (ν_{sym}) and

dx.doi.org/10.1021/ja411583f | J. Am. Chem. Soc. 2014, 136, 2538−2545

asymmetric (ν_{asym}) C−H stretching frequencies appear at 2850 and 2920 cm^{-1}, respectively, which upon melting, shift to 2856 and 2928 cm^{-1}, respectively.[20] Thus, monitoring these peaks as a function of temperature has often been used to follow the phase transitions associated with a variety of systems carrying long-chain hydrocarbons.[21]

In Figure 7, we have plotted the relevant region of the IR spectra of PE-MP-F, along with the variation of the ν_{sym} and

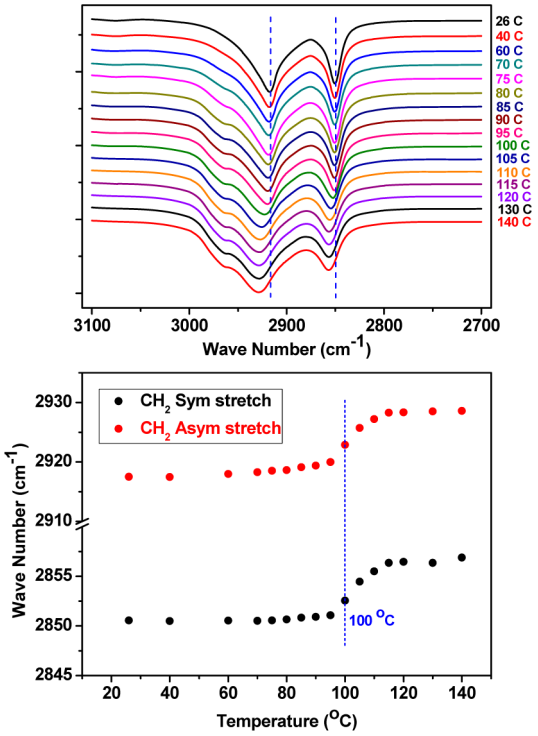

Figure 7. Variable temperature IR spectra of the C−H stretching region of PE-MP-F that is sensitive to conformation of the polymethylene segment; the variation of the ν_{sym} and ν_{asym} C−H stretching vibrations is plotted as a function of temperature in the bottom panel.

ν_{asym} C−H stretching frequencies, as a function of sample temperature. It is noticed that both of these peak positions remain unchanged until ∼95 °C, begin to shift to higher frequency immediately thereafter, and finally level off at ∼115 °C; the net shift in the ν_{sym} occurs from 2851 to 2857 cm^{-1}, while the ν_{asym} peak shifts from 2919 to 2929 cm^{-1}. The onset of this shift in peak positions matches well with the DSC endotherm (at ∼98 °C), which was ascribed to the melting of the HC domain; this change continues until the sample temperature is 115 °C, which is well beyond the second peak ascribed to the melting of FC domain. These measurements were performed by heating the sample and allowing for equilibration at each temperature prior to acquiring the data; it is clear that the population of gauche defects in the all-trans polymethylene segment within the crystalline lattice begins to increase immediately after the melting of the HC domain but attains a near liquid-like conformation only after the isotropization temperature, i.e., after the FC domain has also melted. Similar variable temperature IR studies were also carried out with the PE-DP-F and PE-MP-F samples (Figure S11, Supporting Information); interestingly, in the case of PE-DP-F no abrupt change in the peak positions was observed as one transcends the HC melting peak, but instead the change occurred only near the second clearing transition. Furthermore, the peak positions of the ν_{sym} and ν_{asym} C−H stretching vibrations even at RT were at higher frequencies, viz., 2853 and 2921 cm^{-1}, respectively; this suggests the presence of higher disorder in the crystalline HC phase due to a larger population of gauche defects.[20] This observation is consistent with the significantly lower value of the normalized ΔH_m associated with the HC melting peak in PE-DP-F compared to that for PE-MP-F (57 mJ/mg compared to 100 mJ/mg); furthermore, the distinctly broader peak in the WAXS profile for PE-DP-F with a considerably larger *d*-spacing of 0.476 nm also reflects the poor packing of the alkyl chains within the crystalline lattice of the HC domain. Considering the substantially higher cross-sectional area for the fluoroalkyl chains when compared to alkyl chains (28.3 $Å^2$ and 18.9 $Å^2$, respectively),[16] and the presence of two such chains per repeat unit in PE-DP-F, the crystalline packing within the FC layer would clearly preclude the close packing of the all-trans alkyl chains in the HC layer, and consequently it would lead to higher levels of disorder. In the PE-AP-F sample, on the other hand, a change in both of the C−H stretching frequencies occurred clearly in a short span of 65−75 °C, which corresponds to the single melting peak in the DSC of the sample. In summary, the variable temperature IR spectroscopic studies have helped to reveal the molecular structural changes associated with the thermal transitions observed in the DSC; these are consistent with the findings from the SAXS and WAXS studies and has provided a clearer understanding of the origins for the formation of smectic mesophases in these systems.

■ CONCLUSIONS

The periodically clickable polyethylene-like polyesters described in this study have provided a unique opportunity to place one or two fluoroalkyl chains at regular intervals along the backbone. Using a range of techniques, namely DSC, SAXS, WAXS, TEM, and IR spectroscopy, it was demonstrated that polyethylene-like polyester chains, carrying long-chain alkylene (C18) segments along the backbone and $CF_3(CF_2)_7CH_2CH_2$ (F8C2) pendant units, adopt a folded zigzag conformation whereby the backbone alkylene (HC) segment becomes colocated at the center and is flanked by the perfluoroalkyl (FC) groups on either side, as depicted in Scheme 2. These folded chains then organize into an alternating lamellar structure, permitting the independent crystallization of both the HC and FC segments; on heating, the melting of the HC domains occurs first, inducing substantial fluidity to the matrix and thereby generating a smectic-type mesophase, as confirmed by polarizing light microscopic observations and variable temperature SAXS studies. When each repeat unit of the polymer carries a single pendant fluoroalkyl segment, the organization within both the HC and FC domain occurs efficiently; however, when two pendant fluoroalkyl chains are installed on each repeat unit, the crystallization within the FC domain occurs very effectively but it hinders the optimal organization within the HC domain. The substantially larger cross-sectional area of the fluoroalkyl chains clearly leaves a lot more volume than can be filled by the close packing of all-trans alkylene segments. This is reflected by the absence of a sharp WAXS peak in this sample corresponding to the close packing of alkyl chains and also by the presence of a larger population of gauche defects in the alkylene chains, as evident from their IR spectra. In contrast to earlier reports on polyethylene-like polymers, which were periodically disrupted primarily to

dx.doi.org/10.1021/ja411583f | J. Am. Chem. Soc. 2014, 136, 2538−2545

regulate the lamellar structure, our study proposes an alternate strategy whereby intersegment immiscibility drives individual polymer chains to fold in a zigzag fashion which, due to the crystallization of the backbone alkylene segment, is further stabilized to generate single-chain nanoparticle-like entities. This concept evidently can be elaborated to include other immiscible segments (using simple click reactions), such as biologically relevant hydrophilic moieties, to generate stable single-chain nanoparticles in aqueous solution. Although an interesting polyethylene-like polyester bearing periodically located orthogonally clickable propargyl and allyl moieties was also synthesized, once the fluoroalkyl chains were installed using the propargyl groups, the allyl units appeared to be inaccessible for thiol−ene reaction with PEG-thiols. Alternate schemes or reaction conditions need to be developed to place three mutually immiscible units at well-defined locations within a polymer chain; these types of systems could present unique morphological features. One interesting feature of the observed lamellar morphology is the very small domain size, typically in the range of ∼5−6 nm, which is far smaller than those formed using block copolymers. Thus, these systems can be used to create novel and interesting nanoscale morphologies, at significantly smaller length scales than are usually accessible. Furthermore, it opens up the possibility of generating a variety of other novel periodically layered materials by suitable design of the backbone and pendant segments.

■ ASSOCIATED CONTENT

Supporting Information

Detailed experimental methods, additional NMR spectra, DSC thermograms, SAXS, WAXS, PLM images, and TEM images. This material is available free of charge via the Internet at http://pubs.acs.org.

■ AUTHOR INFORMATION

Corresponding Author

raman@ipc.iisc.ernet.in

Notes

The authors declare no competing financial interest.

■ ACKNOWLEDGMENTS

We thank the Department of Science and Technology, New Delhi, for the J. C. Bose fellowship (2011−2016) to S.R., and Spectroscopy and Analytical Testing Facilities (SATF) for IISc DSC data. J.M. acknowledges CSIR, New Delhi, for the fellowship. We also thank Subi George and Ankit Jain (JNCASR) for carrying out the GPC analysis and S. Vasudevan (IISc) and Bhoje Gowd (NIIST) for their valuable suggestions regarding the variable temperature IR spectroscopy and X-ray scattering studies.

■ REFERENCES

(1) (a) Hadjichristidis, N.; Pispas, S.; Floudas, G. *Block copolymers: Synthetic strategies, Physical properties, and Applications*; Wiley-Interscience: New York, 2003. (b) Ishizone, T.; and Hirao, A. Anionic Polymerization: Recent Advances. In *Synthesis of Polymers: New Structures and Methods*;Schluter, A. D.; Hawker, C. J.; Sakamoto, J., Eds.; Wiley-VCH: Weinheim, 2012; p 81.

(2) Matyjaszewski, K. *Prog. Polym. Sci.* **2005**, *30*, 858.

(3) For recent reviews on graft copolymers, see: (a) Feng, C.; Li, Y.; Yang, D.; Hu, J.; Zhang, X.; Huang, X. *Chem. Soc. Rev* **2011**, *40*, 1282. (b) Uhrig, D.; Mays, J. W. *Polym. Chem.* **2011**, *2*, 69.

(4) Iatrou, H.; Mays, J. W.; Hadjichristidis, N. *Macromolecules* **1998**, *31*, 6697. (b) Paraskeva, S.; Hadjichristidis, N. *J. Polym. Sci., Part A: Polym. Chem.* **2000**, *38*, 931. (c) Uhrig, D.; Mays, J. W. *Macromolecules* **2002**, *35*, 7182. (d) Hirao, A.; Watanabe, T.; Kurokawa, R. *Macromolecules* **2009**, *42*, 3973.

(5) (a) Pfeifer, S.; Lutz, J.-F. *J. Am. Chem. Soc.* **2007**, *129*, 9542. (b) Badi, N.; Lutz, J.-F. *Chem. Soc. Rev.* **2009**, *38*, 3383. (c) Zamfir, M.; Lutz, J.-F. *Nat. Commun.* **2012**, *3*, 1138. (d) Ouchi, M.; Terashima, T.; Sawamoto, M. *Chem. Rev.* **2009**, *109*, 4963. (e) Satoh, K.; Ozawa, S.; Mizutani, M.; Nagai, K.; Kamigaito, M. *Nat. Commun.* **2010**, *1*, 6.

(6) (a) Wagener, K. B.; Valenti, D. *Macromolecules* **1997**, *30*, 6688. (b) Smith, J. A.; Brzezinska, K. R.; Valenti, D.; Wagener, K. B. *Macromolecules* **2000**, *33*, 3781.

(7) Ungar, G.; Zeng, K. B. *Chem. Rev.* **2001**, *101*, 4157.

(8) (a) Alamo, R. G.; Jeon, K.; Smith, R. L.; Boz, E.; Wagener, K. B.; Bockstaller, M. R. *Macromolecules* **2008**, *41*, 7141. (b) Berda, E. B.; Lande, R. E.; Wagener, K. B. *Macromolecules* **2007**, *40*, 8547. (c) Ortmann, P.; Trzaskowski, J.; Krumova, M.; Mecking, S. *ACS Macro Lett.* **2013**, *2*, 125.

(9) (a) Le Fevere de Ten Hove, C.; Penelle, J.; Ivanov, D. A.; Jonas, A. M. *Nat. Mater.* **2004**, *3*, 33. (b) Menges, M. G.; Penelle, J.; Le Fevere de Ten Hove, C.; Jonas, A. M.; Schmidt-Rohr, K. *Macromolecules* **2007**, *40*, 8714.

(10) Roy, R. K.; Gowd, E. B.; Ramakrishnan, S. *Macromolecules* **2012**, *45*, 3063.

(11) (a) Russell, T. P.; Rabolt, J. F.; Twieg, R. J.; Siemens, R. L. *Macromolecules* **1986**, *19*, 1135. (b) Fujiwara, M.; Satoh, K.; Kondo, S.; Ujiie, S. *Macromolecules* **2006**, *39*, 5836. (c) Mahler, W.; Guillon, D.; Skoulios, A. *Mol. Cryst. Liq. Cryst. Lett.* **1985**, *2*, 111. (d) Hopken, J.; Möller, M. *Macromolecules* **1992**, *25*, 2482.

(12) (a) Wilson, L. M.; Griffin. *A. C. Macromolecules* **1993**, *26*, 6312. (b) Wang, J.; Mao, G.; Ober, C. K.; Kramer, E. J. *Macromolecules* **1997**, *30*, 1906. (c) Arehart, S. V.; Pugh, C. *J. Am. Chem. Soc.* **1997**, *119*, 3027.

(13) (a) Wilson, L. M.; Griffin, A. C. *Macromolecules* **1994**, *27*, 1928. (b) Wilson, L. M.; Griffin, A. C. *Macromolecules* **1994**, *27*, 4611.

(14) Volkov, V. V.; Plate, N. A.; Takahara, A.; Kajiyama, T.; Amaya, N.; Murata, Y. *Polymer* **1992**, *33*, 1316.

(15) Bunn, C. W.; Howells, E. R. *Nature* **1954**, *174*, 549.

(16) (a) Dalvi, V. H.; Rossky, P. J. *Proc. Natl. Acad. Sci., U.S.A.* **2010**, *107*, 13603. (b) Wang, J.; Ober, C. K. *Macromolecules* **1997**, *30*, 7560.

(17) (a) Guillaume de, C.; Fabre, P.; Corpart, J. M.; Leibler, L. *Science* **1999**, *285*, 1246. (b) Li, X.; Andruzzi, L.; Chiellini, E.; Galli, G.; Ober, C. K.; Hexemer, A.; Kramer, E. J.; Fischer, D. A. *Macromolecules* **2002**, *35*, 8078.

(18) (a) Yokota, K.; Hirabayashi, T. *Polym. J.* **1985**, *17*, 991. (b) Shimizu, T.; Tanaka, Y.; Kutsumizu, S.; Yano, S. *Macromol. Symp.* **1994**, *82*, 173. (c) Shimizu, T.; Tanaka, Y.; Kutsumizu, S.; Yano, S. *Macromolecules* **1993**, *26*, 6694. (d) Wilson, L. M. *Liq. Cryst.* **1995**, *18*, 347.

(19) Wilson, L. M.; Stuhn, B.; Rennie, A. R. *Liq. Cryst.* **1995**, *18*, 923.

(20) (a) Snyder, R. G.; Strauss, H. L.; Elliger, C. A. *J. Phys. Chem.* **1982**, *86*, 5145. (b) MacPhail, R. A.; Straus, H. L.; Snyder, R. G.; Elliger, C. A. *J. Phys. Chem.* **1984**, *88*, 334.

(21) (a) Barman, S.; Venkataraman, N. V.; Vasudevan, S.; Seshadri, R. *J. Phys. Chem. B* **2003**, *107*, 203. (b) Suresh, R.; Venkataraman, N.; Vasudevan, S.; Ramanathan, K. V. *J. Phys. Chem. C* **2007**, *111*, 495. (c) Manner, W. L.; Bishop, A. R.; Girolami, G. S.; Nuzzo, R. G. *J. Phys. Chem. B* **1998**, *102*, 8816. (d) Fosser, K. A.; Kang, J. H.; Nuzzo, R. G.; Wöll, C. *J. Chem. Phys.* **2007**, *126*, 194707.